Iranian Polymer Journal (2020) 29:957–974
https://doi.org/10.1007/s13726-020-00854-0

ORIGINAL RESEARCH

# Effect of mineral fillers on physico-mechanical properties and heat conductivity of carbon black-filled SBR/butadiene rubber composite

**Mehdi Shiva**[1,2] · **Seyyede Saeede Akhtari**[3] · **Masoud Shayesteh**[3]

Received: 2 December 2019 / Accepted: 2 August 2020 / Published online: 28 August 2020


## Abstract

Heat conductivity, curing rate and fatigue crack growth properties of carbon black-filled styrene butadiene rubber (SBR)/butadiene rubber (BR) blend that is frequently used in passenger car tire treads were simultaneously improved by a hybrid filler system of carbon black, high dispersible precipitated silica, modified layered silicate and ultra-light mixed filler of alumina and aluminum sulfate. An optimum formulation was obtained and a study of mechanisms governing composite properties has been performed according to the filler variables through the designing of experiments and the regression and statistical analysis and with the aid of composite characterization techniques such as dynamic mechanical analysis (DMA) and FE-SEM/EDX. Alumina could improve thermal conductivity, DeMatia crack growth, and the tensile strength of the rubber composite, along with relative maintenance of hardness and modulus. The effects of statistically significant interactions between silica and alumina on the abrasion behavior and thermal conductivity were observed, which was attributed to the presence of the silane coupling agent and the effect of modifying the alumina surface with the ethoxysilanes groups. The partial substitution of carbon black by high dispersible silica resulted in an increase in thermal diffusion coefficient, the improvement of heat buildup, resilience and DeMatia crack growth, and relative maintaining of tensile properties as well as a slight loss in abrasion and aging behavior of the tire tread composite. Through the increase of thermal diffusivity coefficient and a slightly improvement in the aging behavior, modified layered silicate (organoclay) caused a significant reduction in the optimum curing time of the tire tread composite. Some evidence has been provided for the interactions between modified layered silicate and silane coupling agent. The improvement in crack growth and thermal conductivity of the elastomer composite was attributed to smaller interparticle distances of hybrid filler system compared to those of carbon black filler system.

**Keywords** Transport phenomena · Thermal diffusivity coefficient · Tire tread composite · Silane coupling agent · Failure properties

## Introduction

Heat conductivity is one of the most important properties of elastomers in influencing their vulcanization behavior, productivity and quality. It is expected that by increasing rubber heat conductivity, its curing process is improved which is economically significant. Low thermal conductivity of polymers is attributed to their low atomic density, weak interactions or chemical coupling, complex crystal structure and high anharmonicity in their molecular vibrations [1, 2]. The thermal conductivity is the result of an expansion of thermal wave in the direction of temperature gradient that is passed from one molecule to another [3, 4]. Phonon transport is considered to be the main mechanism of thermal conductivity in most polymers [1, 3]. Guo et al. have recently reviewed factors affecting thermal conductivity of

**Electronic supplementary material** The online version of this article (https://doi.org/10.1007/s13726-020-00854-0) contains supplementary material, which is available to authorized users.

✉ Seyyede Saeede Akhtari
ss_akhtari@yahoo.com

[1] Department of Chemical Engineering, Birjand University of Technology, P. O. Box: 97198-66981, Birjand, Iran

[2] Department of Research and Technology, Kavir Tire Co., P. O. Box 518, Birjand, Iran

[3] Department of Chemical Engineering, University of Sistan and Baluchestan, P. O. Box 98155-987, Zaheden, Iran

polymers and polymer composites [4]. They stated that limited understanding of heat transfer in polymer composites imposes restrictions on the design and fabrication of better thermally conductive polymers and polymer composites [4].

Thermal conductivity of polymers and rubbers is improved by adding fillers such as carbon black, graphite, graphene, carbon fiber, nanodiamond, metal particles and metal oxides [1, 3]. However, the amount of filler, the method of filler incorporation, the state of filler dispersion and its alignment as well as the filler/rubber interactions are critical factors affecting the ultimate heat conductivity of a filled rubber composite [4]. In addition, the development of the formula in rubber parts requires consideration of a wide range of engineering properties. It would be worth noting that today there is a growing tendency to use environmentally friendly fillers in polymer and rubber composites. Therefore, the choice of useful filler for polymer and rubber should be considered from several technical and environmental aspects. Concerning the case of a technical piece such as tire tread, this issue becomes more complicated. Carbon black is a classical reinforcing filler for most rubber composites, including tire treads. But the use of this filler is environmentally challenging. Precipitated silica, modified layered silicates and alumina are addressed as environmentally friendly mineral fillers and potential alternatives to carbon black in rubber composites such as tire tread [5]. The compatibility of mineral fillers with polymer matrix can increase by their modifications [5, 6]. Today, highly dispersible precipitated silica is widely used along with silane coupling agents which enhance dynamic performance of polymer composites, including tire tread [7, 8]. Highly dispersible silica gives greater amount of available surface which is the result of better dispersion in rubber matrix. Therefore, the improvement in filler/rubber interactions results in the improvement of the final properties such as tread wear resistance, tear resistance, rolling resistance and wet grip of the tire [9, 10].

The structure, preparation and thermal and mechanical properties of modified layered silicate or organoclay (nanoclay) as fillers within the rubber polymer matrix have been well reviewed [11, 12]. Nanotechnology is an interesting area of research due to its cost-effectiveness and ease of access to natural resources [11]. Kim et al. developed a ternary hybrid filler system including carbon black, silica and modified layered silica in styrene butadiene rubber that showed the most excellent dynamic viscoelasticity, abrasion resistance and mechanical properties, which is considered to be the excellent tire tread composite for passenger cars [13]. In addition, one of the significant features of modified layered silicates, in particular those modified with ammonium salts, is their increasing impact on the rate of sulfur curing of rubbers [14, 15]. Thermal conductivity of polymers is increased using alumina as filler [16, 17]. The use of this filler in rubbers, along with surface modification agents, as the competitor of carbon black and silica has been addressed in a number of articles but requires further study [18, 19]. Li et al. reported thermally conductive emulsion styrene butadiene rubber (ESBR) composites filled with alumina particles [16]. Wang et al. showed that alumina can greatly enhance thermal conductivity, and meanwhile, it performs well in the reinforcing EPDM rubber [17]. A surface modification mechanism of alumina with silane coupling agent was reported similar to that of silica [17, 20].

Carbon black is nanostructured it, i.e., is made by aggregates of spherical primary nanoparticles that cannot be separated by thermomechanical mixing [11]. Highly dispersible precipitated silica is also a nanostructure filler. On the contrary, as the most important novelty in the rubber field, nanofillers such as organoclay and nanosized alumina have primary particles with at least one dimension below 100 nm that can be individually dispersed in the rubber matrix [11]. However, as already stated by Galimberti et al. currently it is clear that in large-scale applications such as tyre treads, nanofillers can hardly replace the nanostructured fillers [11]. So, the combination of both families of fillers can lead to some remarkable properties. The challenging goal of the research activity on hybrid filler systems is to develop synergistic effects between different fillers to achieve substantial improvement of material properties such as different properties of tyre treads that should be balanced [11].

While, the potential of a hybrid system of nanostructure fillers such as silica/carbon black [9, 10] and carbon black/silica/*meta*-kaolin [21] as well as a hybrid system of nanostructure fillers and nanofillers such as carbon black/modified layered silicates [11] and silica/carbon black/modified layered silicates [13] in SBR-based tire tread formulations has been well addressed, but so far the use of a quaternary hybrid filler system, alumina in ternary system and the interaction and synergism effects of these fillers on different properties of tire tread composite has not been investigated. In addition, based on literature review of organoclay application in rubber technology, no direct thermal conductivity improvement of elastomer composite has been reported in gum stocks when it is employed as a single filler or in the presence of carbon black as binary filler. As it is the same for silica application in elastomer composite [22], it should be of immense interest to study silica and organoclay synergistic effects on thermal conductivity of carbon black-filled rubber composites in the presence of more conductive fillers such as alumina.

In this research, we have studied the potential of increasing thermal conductivity and improving mechanical properties of carbon black-filled tire tread composite in the presence of highly dispersible silica, modified layered silicate and an ultra-light alumina-aluminum sulfate filler.

## Experimental

### Materials

*cis*-Butadiene rubber (BR) with a Mooney viscosity of 45–47 (ML1 + 4 at 100 °C) and a density of 0.9 g/cm$^3$ was provided by Arak Petrochemical Co. Styrene butadiene rubber (SBR) with a Mooney viscosity of 46–49 (ML1 + 4 at 100 °C) and a density of 0.93 g/cm$^3$ was provided by Bandar-Emam Petrochemical Co. Carbon black N339 was supplied by Carbon Iran Co., and aromatic oil was also provided by Behran Oil Co. The modified layered silicate (organoclay) used was kindly supplied by Kava Sannat Payvar Co. of Iran with a pycnometer density of 1.07 g/cm$^3$ and pH 6.19. This filler is the product of the treated and surface modified montmorillonite minerals that was obtained from the bentonite mines of South Khorasan, Iran, whose composition is similar to Cloisite 30B. Ultra-light alumina-aluminum sulfate filler with a pH of 3.57, a density (toluene solvent) of 0.93 g/cm$^3$ and a pour density of 0.037 g/cm$^3$ was purchased from Iran Azarshahr Research Center and prepared by spray pyrolysis method from treatment of nepheline syenite mineral with sulfuric acid and aluminum sulfate-18-hydrate precursor. The FTIR, XRD and SEM characteristics of this kind of alumina as well as those of the used organoclay are presented in Supplementary Material. Highly dispersible silica (HDS) with a commercial name of silica W/C 1165MP and with pH of 6.7, Brunauer Emmet Teller (BET) surface of 165 m$^2$/g, pycnometer density of 2.06 g/cm$^3$, cetyl trimethyl ammonium bromide (CTAB) surface area of 156 m$^2$/g and dibutyl phthalate (DBP) absorption of 235 mL/100 g was obtained from Huang Yan ZheDong Co. Bis (triethoxysilylpropyl) tetrasulfide (TESPT) or Si69 silane coupling agent was purchased from the Degussa Corporation. Other materials including sulfonamide and guanidines accelerators, anti-degradants, stearic acid, zinc oxide and sulfur were supplied by Ding Yuan Co. (China), Shandong Sunsine Co. (China), Southern Acids Co. (Malaysia), Sepid Oxide Shokuhieh Co. (Iran) and Teskdoc Iran Co., respectively.

### Preparation of rubber composite

The base formula used is a blend of styrene-butadiene and *cis*-butadiene rubber filled with carbon black. The carbon black amount is 53 phr and the total amount of oil in the formula is equivalent to 27 phr. Zinc oxide, stearic acid, accelerator, sulfur, antioxidant and anti-ozonant agents are other materials added to the radial passenger tire tread formulations (Table 1). Three factors two levels full factorial design of experiments (FFDOE) were used to study the effect of modified layered silicates, precipitated silica and alumina incorporation into the base formula. Variable levels were selected as follows:

High dispersible silica (HDS): 0 and 20 phr.

Alumina (AL): 0 and 3 phr.

Modified layered silicate (OC): 0 and 1 phr.

For the two-level three factorial experimental designs, a total number of eight experimental runs, shown in Table 1 were performed. The composite marked with Mix5 is the carbon black-filled reference formula. In the above design, silica was used as an alternative in an amount equivalent to the amount of carbon black. However, organoclay and aluminum additives were added to the formula without reducing carbon black. The DPG accelerator and silane coupling agent were also used in the formulations containing silica. Concerning the weight, the amount of silane was equivalent to 10% of used silica and the diphenylguanidine accelerator (DPG) amount was equivalent to 2% of used silica. The composites were prepared by adding rubbers, chemicals (antioxidant, antiozonants, stearic acid and zinc oxide), fillers and oil under the same conditions and according to the specified instructions in a 2-l internal mixer of tangential type (Pomini, Italy). The mixer rotor speed was selected at 40 rpm and the discharge temperature was 150 °C. The composites were finalized on a two-roll mill (under the condition of 50–60 °C roll surface temperature and 40 rpm of rotor speed) by adding sulfur and accelerators. Two mixtures were prepared and characterized for each composition.

**Table 1** Formulation of samples

| Code | Highly dispersible silica HDS (phr) | Alumina, aluminum sulfate AL (phr) | Organoclay OC (phr) |
|---|---|---|---|
| Mix1 | 0 | 0 | 1 |
| Mix2 | 0 | 3 | 1 |
| Mix3 | 0 | 3 | 0 |
| Mix4 | 20 | 0 | 0 |
| Mix5 | 0 | 0 | 0 |
| Mix6 | 20 | 3 | 0 |
| Mix7 | 20 | 3 | 1 |
| Mix8 | 20 | 0 | 1 |

Styrene butadiene rubber (SBR): 85 phr; *cis*-butadiene rubber (BR): 15phr; carbon black: 53 phr; oil: 27 phr; HDS: 0 or 20 phr; TESPT: 0 or 2 phr; activators: 3.3 phr; protectors: 3 phr; accelerators: 1.3 phr; DPG: 0 or 0.4 phr; sulfur: 1.5 phr; PVI: 0.1 phr

### Characterization

The density of uncured rubber composites was measured by a Brabender Elatest rubber composite density measuring

device (Germany). Curing properties include optimal curing time (T90), scorch time (TS2), minimum torque (ML), maximum torque (MH), delta torque (DH) and curing rate (Pr) were measured at 145 °C for 45 min by an oscillating die rheometer (ODR 2000 E, Alpha technologies). To investigate the thermal and mechanical properties of rubber composites (after 24 h of storage) they were vulcanized at 145 °C in a 20-ton curing press device. The vulcanization time of the composites corresponded with optimum cure time (T90) derived from curing curves of ODR 2000E. The tensile stress (TS), elongation-at-break (EAB) and modulus (M300) of rubber composites were determined as per ASTM D412 using a tensile tester device (5–10 K-S, Hounsfield, UK) and standard dumb-bell test pieces.

The DeMatia crack growth rate (DCG) was measured by a flexing fatigue tester (Hounsfield, UK). Abrasion was determined by a DIN abrasion tester (Zwick 6104-H04, Germany) according to ISO 4649. The total volume loss of samples was reported. The hardness of vulcanizates was measured using a Shore-A durometer (Zwick 3100, Germany) according to ASTM D2240. The resilience of vulcanizates was determined by Wallace UK Dunlop Tripsometer $R^2$ according to DIN 53512. A Goodrich flexometer (FT-1110, Ueshima Seisakusho Co., Japan) was used to test the heat buildup of cylindrical specimens. The final sample temperature was reported after 30 min from the start of the test. To determine the aging behavior of composites, the dumb-bell shape samples of tensile test were placed at 100 °C for 72 h and the tensile behavior was measured before and after aging. Then, the aging coefficient ($K$) was calculated according to the formula presented by Pan et al. [23] (Eq. 1):

$$K = \frac{f}{f_0}, \tag{1}$$

where $K$ is the aging coefficient, $f_0$ and $f$ are the performance functions before and after aging conditions, in which $f$ and $f_0$ are obtained from the following equation:

$$f = \mathrm{EAB} \times \mathrm{TS}, \tag{2}$$

where EAB is the elongation-at-break of rubber samples and TS is the tensile strength. The bigger and closer to 1 as value for $K$, the better aging behavior of the rubber sample will be expected [23].

It is important to note that all tests for each composite have been repeated three or four times and the final results are average of data for each property.

To take FE-SEM images, white fillers (alumina, silica, and organoclay) in the absence of carbon black and only in the presence of curing agents (zinc oxide, stearic acid, sulfur and accelerator) were added to the SBR/BR blend on a two-roll mill. The specimen was then cured at 145 °C for 1 h in a suitable mold used to test hardness and resilience. After breaking the sample in liquid nitrogen and gold coating treatment, the hybrid filler morphology (dispersion) in rubber composite was exhibited along with an elemental analysis by field emission scanning electron microscopy (FE-SEM) coupled with energy dispersive X-ray analysis (EDX), MIRA3 FE-SEM/EDX (Tescan, Czech Republic). The structure and dispersion state of fillers in rubber vulcanizates in the presence of carbon black were also studied using an optical microscope, Dispergrader 1000 (Opti-GRADE, Sweden).

The dynamic mechanical property analyses of some vulcanizates were performed by a DMA1 dynamical mechanical analyzer (Mettler Toledo, Switzerland) in tension mode with constant frequency of 1 Hz and sweeping temperature of −70 °C to 70 °C. Test samples were used with the length of 14 mm, the width of 11 mm and the thickness of 1.5 mm.

To study the heat diffusivity behavior, a wire embedded rectangular sample (Fig. 1) with a $5 \times 5 \times 2$ $cm^3$ dimension was cured for each composite. The cured samples were then immersed in a silicon oil bath at temperature of $135 \pm 2$ °C. The temperature change of a point at the center of the samples was determined using a temperature recorder. In the next step, the temperature–time data were used to calculate the coefficient of thermal diffusion of rubber composite (Alpha) using ABAQUS software. The three-dimensional transient heat conduction equation (Eq. 3) was considered for the problem simulation [24, 25]. In Eq. (3), the sample temperature is based on the time variable ($t$), the location ($x$, $y$, $z$) in the Cartesian coordinates and the thermal diffusion coefficient of the rubber composite obtained from Eq. 4, where $k$ is the thermal conductivity coefficient, $C$ is the thermal capacity and $\rho$ is the density of the rubber composite. After defining the problem in ABAQUS software, a hypothesized amount was considered for heat conduction coefficient and heat capacity, and the problem was solved. The simulated temperature profile in the sample center was compared with the experimental data for the thermocouple

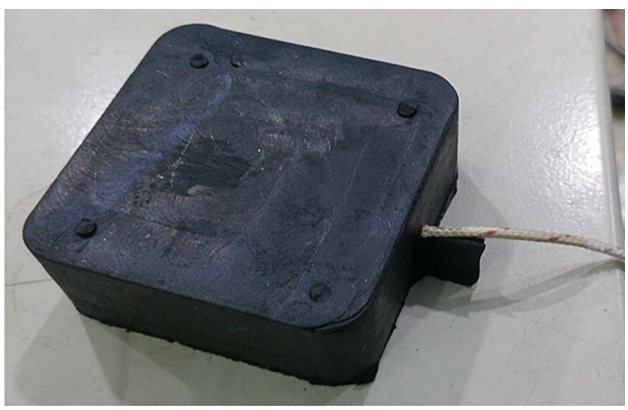

**Fig. 1** Heat diffusivity measurement sample

test for the sample center. This process was repeated with different values of $k$ and $C$ so that the simulation and experimental profiles became as close as possible to each other. The values of $k$ and $C$ which resulted in the best temperature profile were used to calculate $\alpha$:

$$\frac{\partial^2 T(x,y,z,t)}{\partial x^2}+\frac{\partial^2 T(x,y,z,t)}{\partial y^2}+\frac{\partial^2 T(x,y,z,t)}{\partial z^2}=\frac{1}{\alpha}\frac{\partial T(x,y,z,t)}{\partial T} \tag{3}$$

$$\alpha=\frac{k}{\rho C}. \tag{4}$$

## Statistical analysis and development of optimal formulas

Data from full factorial design were used for determining the regression coefficients of first-order model of Eq. (5) [26, 27]:

$$\begin{aligned} Y=&\beta_0+\beta_1\times \mathrm{HDS}+\beta_2\times \mathrm{AL}+\beta_3\times \mathrm{OC}\\ &+\beta_4\times \mathrm{HDS}\times \mathrm{AL}+\beta_5\times \mathrm{HDS}\times \mathrm{OC}\\ &+\beta_6\times \mathrm{AL}\times \mathrm{OC}, \end{aligned} \tag{5}$$

where $Y$ is the predicted response (17 properties in the present study), $\beta_0$ model constant, HDS, OC and AL are the coded value of silica, organoclay and alumina, respectively, $\beta_1$, $\beta_2$ and $\beta_3$ are the linear coefficients and $\beta_4$, $\beta_5$ and $\beta_6$ are the cross product or interaction coefficients. A computer analysis has been done using commercially available package (MINITAB 17) to compute the equation constants ($\beta_0$–$\beta_6$) and their corresponding statistics. Fisher's analysis was used to examine the statistical significance of the developed models. The confidence level was 90%. The importance of the statistical model in MINITAB software is investigated based on $P$ statistics. If $P$ calculated for a model is $< 0.1$ ($P$ model $< 0.1$), then this model is statistically significant. In the MINITAB software, $P$ statistics are also used to check the importance of each factor in the model. If the value of $P$ for each coefficient is $< 0.1$, then the coefficient is statistically significant. Finally, a multi-objective optimization approach has been used in MINITAB17 software to develop an optimum formula based on regression models.

# Results and discussion

## Filler dispersion

Figure 2 shows the FE-SEM images related to dispersion of hybrid filler system (HDS, AL and OC) in SBR/BR based rubber matrix along with an elemental analysis through EDX spectrum. Very fine nanoparticles of alumina are hardly detected in elemental mapping images (Fig. 2c) placed next to larger agglomerates. The silica aggregates along with larger agglomerates are also detected. The dispersion of HDS/AL, AL and OC alone in SBR/BR rubber matrix is also presented in Figure S4 of Supplementary Material. Figure 3 presents optical pictures of filler dispersion by Dispergrader in SBR/BR rubber matrix. The good dispersion state of alumina filler system, organoclay filler system, silica/alumina binary filler system, silica/alumina/carbon black ternary filler system and carbon black filler system have been shown in rubber matrix.

## Properties of rubber composite

The formulations of the composites and the properties obtained from the experiments are given in Tables 1 and 2, respectively. The model fitting assessment based on several statistics including the variance, the coefficients of multiple determination ($R^2$ and $R^2_{\mathrm{adj}}$) and analysis of variance $P$ model statistics is presented in Table 3.

In this study, the regression models of the properties with a $P$ value of $< 0.1$ are considered to be statistically significant. They include seven properties: scorch time (TS2), optimal curing time (T90), curing rate (Pr), thermal diffusion coefficient (Alpha), heat buildup (HBU), DeMatia crack growth (DCG) and abrasion. The coefficients of fitted equation for statistically significant properties (responses) and their percent significance in the form of $P$ value are shown in Table 4. Wherever the $P$ statistic is $< 0.1$, the corresponding term is statistically significant at 90% confidence level. The interaction effects curve is plotted for properties with statistically significant interaction terms. For other properties, only the main effects curve is plotted. DOE-based regression models have been also employed by other researchers in rubber compounding studies, for example by Ghasemi et al. [28] and Balachandran et al. [29].

## Density and curing characteristics of composites

The effect of the formula factors on the rubber composite density is shown in Fig. 4. The density of composites increases by changing the formula factors based on the experimental design. This is mainly due to higher particle density of silica (2.1 g/cm$^3$) than carbon black (1.8 g/cm$^3$) and higher particle density of alumina (0.93 g/cm$^3$) and organoclay (1.07 g/cm$^3$) than gum rubber (0.92 g/cm$^3$) as well as the presence of silane coupling agent along with silica. Figure 4 also shows the dependence of the curing properties of the rubber composite including the minimum torque (ML), the maximum torque (MH), the delta torque (DH) and MH-ML to the three variables of silica (HDS),

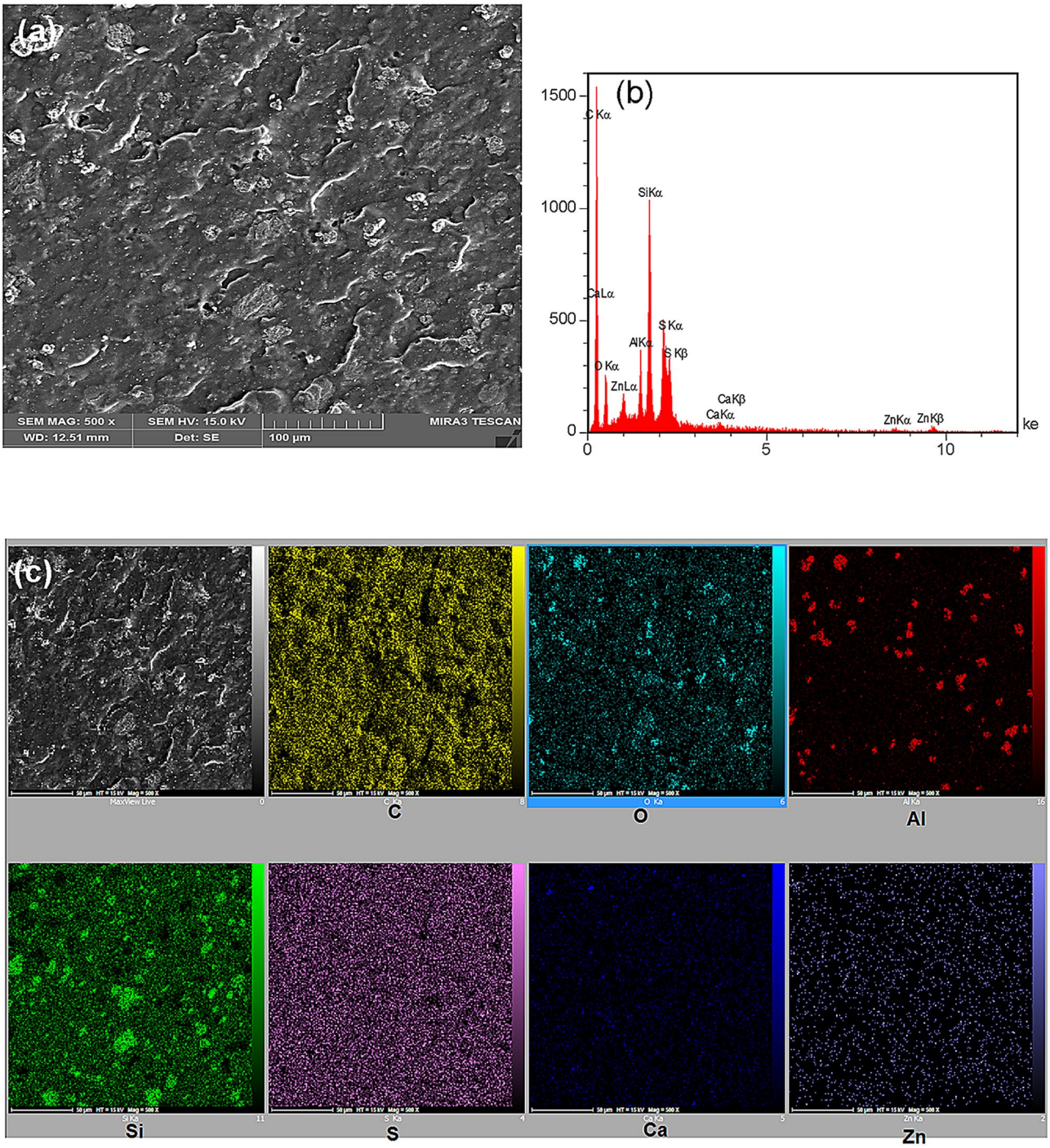


**Fig. 2** **a** FESEM images of HDS/AL/OC ternary hybrid filler system in SBR/BR composite at 500× (**b**) EDX spectrum and (**c**) elemental mapping analysis

alumina (AL) and organoclay (OC) in the form of the main effects curves, which demonstrates that ML decreases by replacing part of the carbon black with silica. On the other hand, the DH increases, so that the MH will eventually be remarkably unchanged. ML increases in the presence of alumina and DH remains unchanged, while MH slightly increases. The reduction of ML (melt viscosity) through partial substitution of carbon black with HDS demonstrates lower filler/rubber interaction of silica compared to carbon black. However, the increase of ML with AL at fixed loading of carbon black may be due to high interactions between alumina particles and rubber chains. After loading 1 phr of

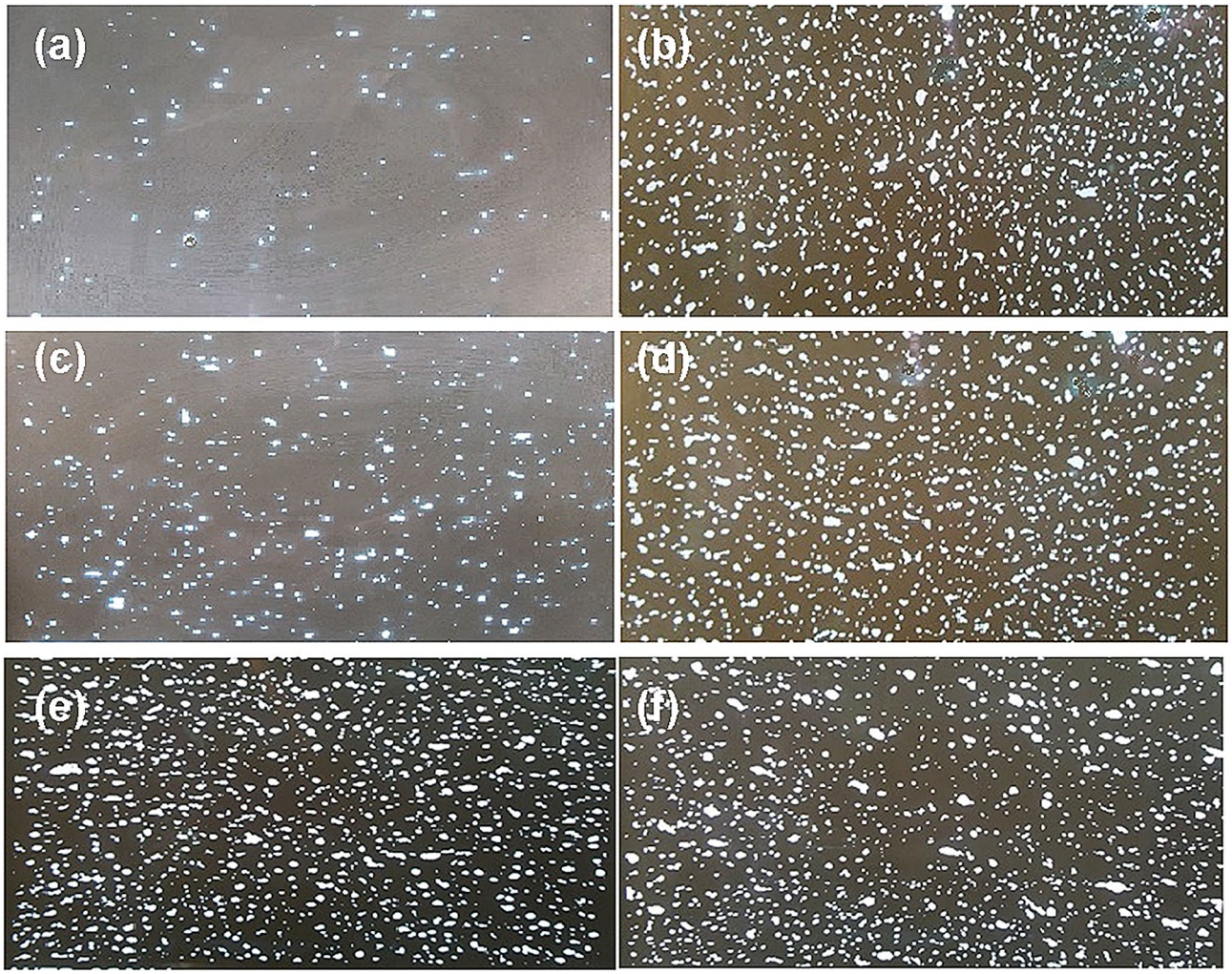


**Fig. 3** Dispergrader pictures of filler dispersion in SBR/BR composite (**a**) gum vulcanizate, (**b**) AL (3 phr), (**c**) OC (3 phr), (**d**) HDS/AL (20/1.5 phr), (**e**) carbon black/HDS/AL (33/20/1.5 phr) and (**f**) carbon black (53 phr)

OC, small changes can be observed in ML, as well as a slight increase in MH and DH indicating a slight increase in sulfur crosslink density.

Enhancement of DH with HDS may be attributed to the increasing effect of silane coupling agent on the crosslink density of the composites, because new covalent bonds may be formed between silica surface and rubber chains through silane bridges during curing period. In addition, every molecule of TESPT contains about four sulfur atoms and elemental sulfur can be detached from the silane coupling agent by heating. In general, the increase in the amount of elemental sulfur in a rubber composite causes the increase of crosslink density and the content of polysulfide crosslinks [30].

Figure 5 shows the interaction effects curve for the three curing properties including TS2, T90 and Pr. Statistical analysis (Table 3) shows that the dependence of all three properties is significant ($P$ values for TS2, T90 and Pr model are 0.032, 0.068 and $0.026 < 0.1$, respectively). Table 4 shows the model coefficients for these three properties. Silica and OC significantly reduce the composite TS2, while alumina shows a minor incremental impact on TS2. Optimum curing time (T90) significantly decreases in the presence of OC, as contrarily, it increases in the presence of alumina. In general, the effect of silica on the optimal curing time is negligible. Pr decreases in the presence of alumina and silica and it increases in the presence of OC. The negative effect of alumina on the curing behavior, which is reflected in the reduction of Pr and the increase of T90 of rubber composite, is related to the acidic nature of these particles. The presence of surface OH groups of alumina has been observed in the FTIR spectrum (Figure S1 in Supplementary Material).

Silica also shows an acidic nature due to the presence of silanol groups. When silica is used alone, the replacement of some of it with carbon black has a negative effect on the curing system of rubber. Using appropriate amounts of the silane coupling agent and mixing them at appropriate

**Table 2** Rheometry properties at 145 °C and other properties

| Properties | Mix 1 | Mix 2 | Mix 3 | Mix 4 | Mix 5 | Mix 6 | Mix 7 | Mix 8 |
|---|---|---|---|---|---|---|---|---|
| Density (g/cm$^3$) | 1.132 | 1.141 | 1.138 | 1.139 | 1.128 | 1.145 | 1.149 | 1.141 |
| ML (Ib-in) | 7.28 | 8.05 | 8.01 | 6.91 | 7.79 | 6.98 | 7.25 | 6.92 |
| MH (Ib-in) | 31.41 | 33.39 | 31.61 | 31.85 | 32.29 | 32.26 | 32.1 | 32.22 |
| DH (Ib-in) | 24.13 | 25.34 | 23.60 | 24.94 | 24.49 | 25.28 | 24.85 | 25.30 |
| TS2 (min) | 9.52 | 9.48 | 11.18 | 9.13 | 11.31 | 9.46 | 9.02 | 8.47 |
| T90 (min) | 21.26 | 22.84 | 28.56 | 24.34 | 26.45 | 28.28 | 25.73 | 23.04 |
| Pr (Ib-in/min) | 3.80 | 3.29 | 2.30 | 3.10 | 2.89 | 2.19 | 2.40 | 3.29 |
| TS (MPa) | 15.26 ± 1.06 | 16.56 ± 0.8 | 15.96 ± 0.6 | 15.50 ± 1.2 | 15.03 ± 0.9 | 16.43 ± 1.1 | 14.46 ± 1.1 | 14.73 ± 0.7 |
| EAB% | 381.9 ± 1.3 | 411.52 ± 0.8 | 395.77 ± 0.6 | 383.16 ± 1.2 | 378.53 ± 0.58 | 422.19 ± 1.3 | 385.74 ± 0.9 | 388.59 ± 0.7 |
| M300 (MPa) | 8.07 ± 0.8 | 8.05 ± 1.05 | 8.15 ± 1.2 | 8.25 ± 0.7 | 8.26 ± 0.4 | 7.7 ± 0.83 | 7.66 ± 1.2 | 7.58 ± 0.66 |
| Aged TS (MPa) | 12.94 ± 0.3 | 12.55 ± 1.1 | 11.41 ± 0.5 | 12.57 ± 0.7 | 13.78 ± 1.1 | 13.38 ± 0.9 | 13.74 ± 1.2 | 12.88 ± 0.6 |
| Aged EAB (%) | 200.16 ± 3.6 | 190.51 ± 2.3 | 215.30 ± 2.1 | 179.99 ± 1.45 | 233.17 ± 3.8 | 148.64 ± 1.3 | 185.10 ± 1.28 | 219.26 ± 3.1 |
| Abrasion (mm$^3$) | 76 ± 0.6 | 105 ± 0.57 | 97 ± 0.9 | 96 ± 1.1 | 80 ± 0.4 | 93 ± 0.5 | 100 ± 0.6 | 90 ± 0.8 |
| Hardness (SHORE A) | 59 ± 1.2 | 60 ± 0.7 | 60 ± 0.6 | 58 ± 0.57 | 60 ± 0.9 | 61 ± 1.05 | 61 ± 0.5 | 60 ± 0.8 |
| *K* | 0.4 | 0.4 | 0.4 | 0.4 | 0.5 | 0.3 | 0.4 | 0.5 |
| DCG (mm/kc) | 0.90 | 0.86 | 0.60 | 0.63 | 0.84 | 0.39 | 0.43 | 0.52 |
| Resilience (%) | 24.9 | 24.9 | 24.9 | 27.1 | 27.1 | 24.9 | 24.9 | 27.1 |
| Alpha($\alpha$) (m$^2$/s) | $2.1\times10^{-7}$ | $2.3\times10^{-7}$ | $1.6\times10^{-7}$ | $2.1\times10^{-7}$ | $1.5\times10^{-7}$ | $2.6\times10^{-7}$ | $2.4\times10^{-7}$ | $1.9\times10^{-7}$ |
| HBU (°C) | 85 | 88 | 87 | 78 | 82 | 84 | 84 | 79 |

*ML* minimum torque, *MH* maximum torque, *DH* delta torque, *TS2* scorch time, *T90* optimum curing time, *Pr* curing rate, *TS* tensile strength, *EAB* elongation-at-break, *DCG* DeMatia crack growth, *HBU* heat buildup

**Table 3** Statistical analysis results for the properties

| No. | Property | *S* | $R^2$ | $R^2_{adj}$ | *P* model |
|---|---|---|---|---|---|
| 1 | Density | 0.00106 | 99.64 | 97.50 | 0.112 |
| 2 | ML | 0.10253 | 99.36 | 95.45 | 0.150 |
| 3 | MH | 1.12784 | 49.23 | 0.00 | 0.953 |
| 4 | DH | 1.02177 | 62.06 | 0.00 | 0.896 |
| 5 | TS2 | 0.04596 | 99.97 | 99.80 | 0.032 |
| 6 | T90 | 0.25456 | 99.87 | 99.07 | 0.068 |
| 7 | Pr | 0.02121 | 99.98 | 99.86 | 0.026 |
| 8 | TS | 0.55508 | 92.58 | 48.06 | 0.486 |
| 9 | EAB | 19.18380 | 78.39 | 0.00 | 0.754 |
| 10 | M300 | 0.19092 | 93.15 | 52.06 | 0.469 |
| 11 | *K* | 0.03536 | 95.65 | 69.57 | 0.380 |
| 12 | DCG | 0.01768 | 99.89 | 99.21 | 0.063 |
| 14 | Abrasion | 0.35355 | 99.98 | 99.87 | 0.025 |
| 15 | Hardness | 1.06066 | 83.64 | 0.00 | 0.680 |
| 16 | Resilience | 0.77782 | 93.33 | 53.33 | 0.463 |
| 17 | HBU | 0.35355 | 99.86 | 99.00 | 0.071 |
| 18 | Alpha | 0.035355 | 99.88 | 99.14 | 0.066 |

temperature and time conditions, the process of modifying the silica can be accomplished well through the silanization reaction inside the internal mixer [10, 20]. This effect, along with the use of minor amounts of DPG accelerators prevents significant change in curing time and the T90 of the rubber composite in the presence of silica. Guanidine-type accelerators are commonly recommended with a thiazole or sulfonamide primary accelerators [9, 10].

The increasing effect of OC on Pr and its decreasing effect on T90 and TS2 of the rubber composite are due to the alkaline nature of the organoclay produced by modification with ammonium salts. The presence of these surface groups is observed by the FTIR spectrum of OC (Figure S1 in Supplementary Material). The band of 1467 cm$^{-1}$ is assigned to the ammonium salt [14]. Improvement of curing behavior in the presence of OC (ammonium salts-modified montmorillonite) has been addressed in several articles [14, 15].

The interaction plots for TS2 (Fig. 5a), T90 (Fig. 5b) and Pr (Fig. 5c) also show that there is an interaction effect between OC and HDS. The $\beta_5$ coefficient of Eq. 5 is statistically significant for above properties from *P* value < 0.1 of HDS × OC term as presented in Table 4. According to the interaction plots demonstrated in Fig. 5, the rubber composites including 1 phr of OC exhibits a severe decrease of TS2 and T90 and a severe increase of Pr in the absence of HDS (0 phr). However, the slope of the curves decreases in the presence of HDS (20 phr). This effect may also be explained according to the presence of silane coupling agent and its interactions by OC as it has already been addressed by some researchers [5, 31]. Clay which has a surface composed of Si–OH and Al–OH functionalities is capable of covalent bond formation with silane coupling agent [5].

**Table 4** Regression coefficients and statistical significance of the coefficients (Eq. 5)

| | $\beta_0$[a] (*P* value) | $\beta_1$ (*P* value) | $\beta_2$ (*P* value) | $\beta_3$ (*P* value) | $\beta_4$ (*P* value) | $\beta_5$ (*P* value) | $\beta_6$ (*P* value) |
|---|---|---|---|---|---|---|---|
| TS2 | 9.6963 (– 0.001) | – 0.6762 (– 0.015) | 0.0887 (– 0.115) | – 0.5738 (– 0.018) | 0.2625 (– 0.078) | 0.5975 (– 0.035) | 0.0775 (– 0.253) |
| T90 | 25.0625 (0.002) | 0.2850 (0.195) | 1.2900 (0.044) | – 1.8450 (0.031) | 0.3675 (0.153) | 0.8825 (0.065) | – 0.2225 (0.245) |
| Pr | 2.90750 (0.002) | – 0.16250 (0.029) | – 0.36250 (0.013) | 0.28750 (0.017) | – 0.08750 (0.054) | – 0.18750 (0.025) | 0.01250 (0.344) |
| DCG | 0.64625 (0.006) | – 0.15375 (0.026) | – 0.07625 (0.052) | 0.03125 (0.126) | – 0.00625 (0.500) | – 0.04875 (0.081) | 0.04375 (0.090) |
| Abrasion | 92.125 (0.001) | 2.625 (0.030) | 6.625 ( 0.012) | 0.625 (0.126) | – 4.875 ( 0.016) | – 0.375 ( 0.205) | 3.125 ( 0.025) |
| HBU | 83.375 (0.001) | – 2.125 ( 0.037) | 2.375 (0.033) | 0.625 (0.126) | 0.375 (0.205) | – 0.375 (0.205) | – 0.375 (0.205) |
| Alpha | 2.0625 (0.004) | 0.1875 (0.042) | 0.1625 (0.049) | 0.1125 (0.070) | 0.0875 (0.090) | – 0.2125 (0.037) | 0.0125 (0.500) |

[a] $Y = \beta_0 + \beta_1 \times \mathrm{HDS} + \beta_2 \times \mathrm{AL} + \beta_3 \times \mathrm{OC} + \beta_4 \times \mathrm{HDS} \times AL + \beta_5 \times \mathrm{HDS} \times \mathrm{OC} + \beta_6 \times \mathrm{AL} \times \mathrm{OC}$

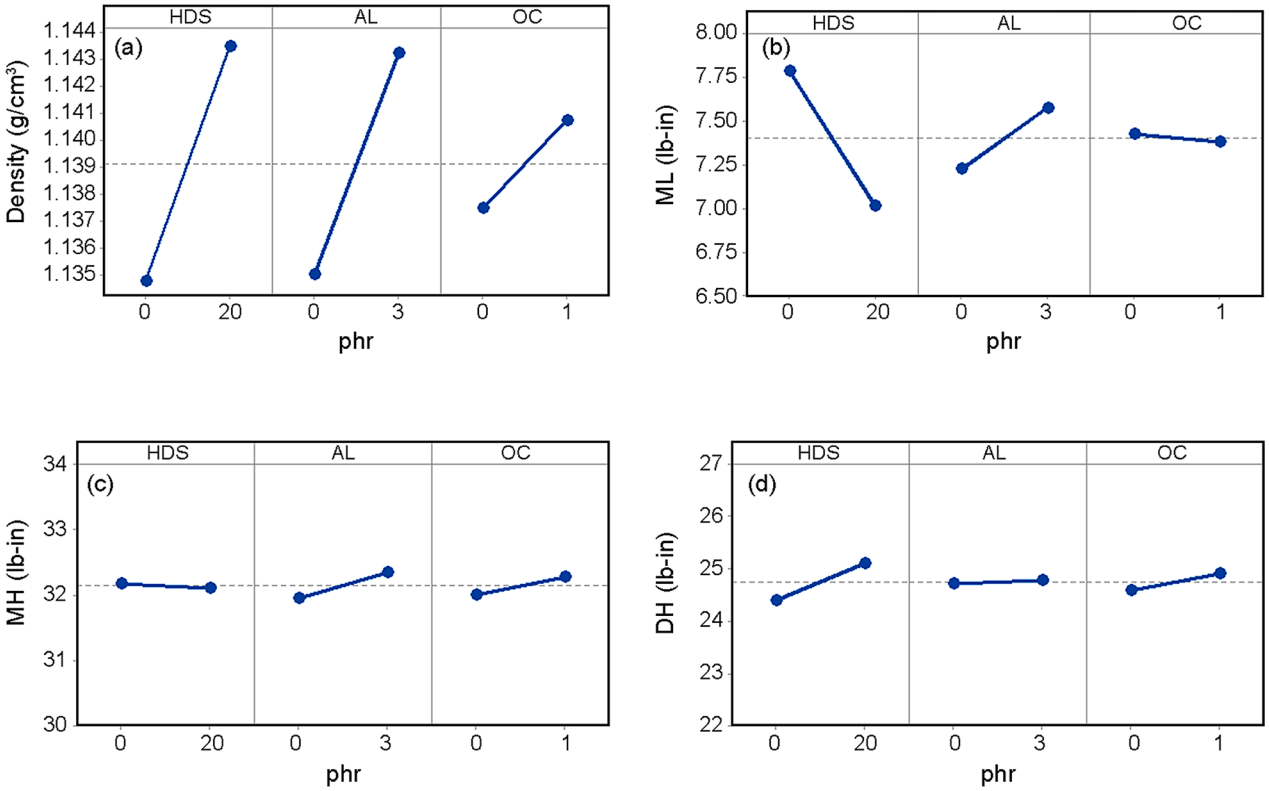


**Fig. 4** Main effects plots of filler concentration for (**a**) density, (**b**) minimum torque (ML), (**c**) maximum torque (MH) and (**d**) delta torque (DH) of rubber composites

Silanol groups on the clay surface and ethoxy group of silane coupling agent interact with the release of ethanol to provide the chemical anchorage on the clay surface [32]. So, the catalytic activity of OC for sulfur curing of rubber may be decreased due the presence of silane macromolecules which are attached to the clay surface and their inhibition effects for quaternary ammonium groups of OC. However, this topic needs further study. The presence of Si–OH group on OC may be confirmed by FTIR (Figure S1 in Supplementary Material). The bands at 3630 $cm^{-1}$ are associated with the

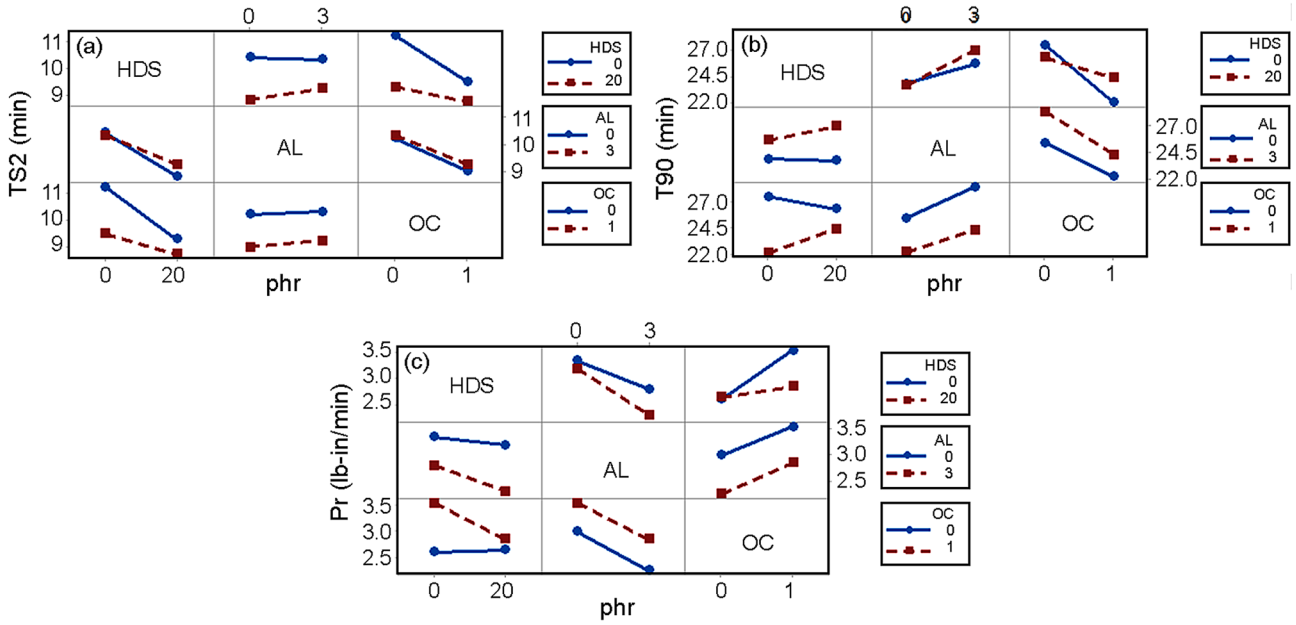


**Fig. 5** Interaction plots of filler concentration for (**a**) scorch time (TS2), (**b**) optimum curing time (T90) and (**c**) curing rate (Pr) of rubber composites

stretching modes of Si–OH group. It is interesting that the interaction effects between HDS and OC have been also presented in other properties such as DCG and HBU which are more sensitive to the changes of sulfur crosslinks (refer to the following sections).

## Hardness and resiliency behavior of rubber composites

The variation of hardness (Shore-A) and rebound resilience with content of HDS, AL and OC is shown in Fig. 6 as main effects plot. The filler loading directly affected the polymer–filler interaction, which in turn, is reflected in the hardness and rebound resilience of composites [7]. In this study, the variation of hardness is the same as the maximum torque variation. Alumina shows an incremental effect on this property. On the other hand, alumina shows a decreasing effect on resilience, while silica shows a slight incremental effect. The greater rebound resilience of the composites in the presence of silica is due to the weaker rubber/filler interaction which meant that less energy was dissipated by friction of the rubber on the filler surface [7]. The hardness main effects plot for silica shows that weaker silica/rubber interaction may be compensated through the increase of crosslink density by adding TESPT to obtain the same hardness as carbon black. The reinforcing effect of AL may

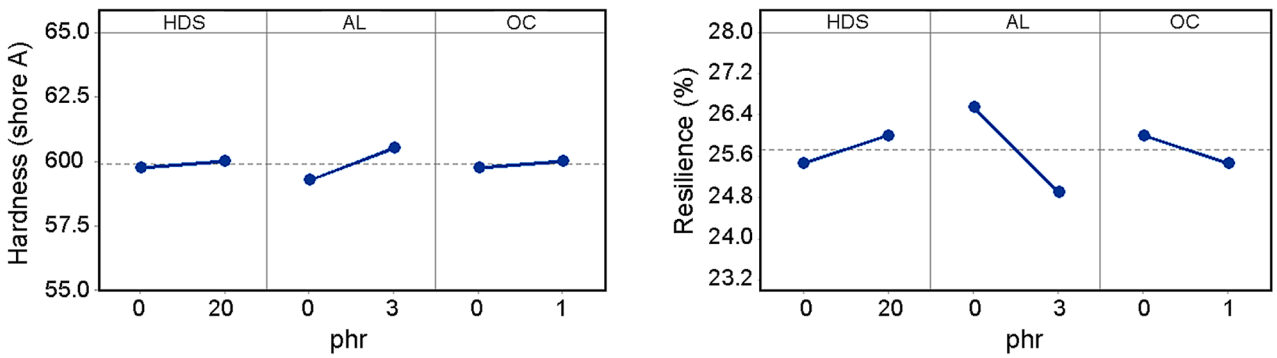


**Fig. 6** Main effects plots of filler concentration for (**a**) hardness and (**b**) resilience of rubber composites

be also confirmed by its increasing effect on the hardness and its decreasing effect on the resilience of the composites. Introduction of reinforcing filler caused the reduction of resilience or the increase of hysteresis due to the energy consumed by polymer/filler friction [7].

## Tensile and aging behavior of rubber composite

The change in tensile properties including tensile strength, elongation-at-break and modulus, as well as aging coefficient ($K$) profiles with respect to HDS, AL and OC contents, as main effects, is shown in Fig. 7. The changes are not great and highly considerable based on statistical analysis (Table 3). However, the presence of alumina seems to cause the increase of tensile strength and elongation-at-break of the composite. All three factors show a slight reduction in rubber composite modulus. According to the tensile and modulus results, HDS shows slightly less reinforcing effects than carbon black. Similar results have been presented by Custodero and Tardivat who have compared the effects of carbon black, high dispersible silica (Z1165) and alumina on mechanical properties of SBR rubber composites [33]. This comparison has been also done by Gherib et al. [34]. Galimberti et al. stated that in SBR-based composites with 60 phr of carbon black, the replacement of carbon black with the same volume fraction of OC (5 and 10 phr) led to the reduction of modulus, elongation-at-break and tensile strength of rubber composite [11]. This study also demonstrated the same results when 1 phr of OC was loaded. As stated by Jeon et al., the decrease in tensile strength by OC can be attributed to the decrease in homogeneity of the composites due to increasing in curing rate (Pr) [35]. The increase in tensile strength by AL can also be addressed through the increase in composite homogeneity as a consequence of the significant decrease in composite curing rate.

As an indirect method, it might be beneficial to study aging coefficient (Fig. 7d) to examine the types of crosslinks in the presence of different fillers. The aging behavior of sulfur-cured rubber composites depends on crosslink distribution. In addition, higher curing rate of rubber composite favors the formation of monosulfide rather than polysulfide bonds, accordingly better aging properties may be obtained [36]. The above results can be interestingly confirmed by comparing the plots of Fig. 5c (curing rate according to the HDS, AL and OC) and Fig. 7d ($K$ according to the HDS, AL and OC); OC shows an improving effect (higher $K$ values) on aging property along with the increase in curing rates,

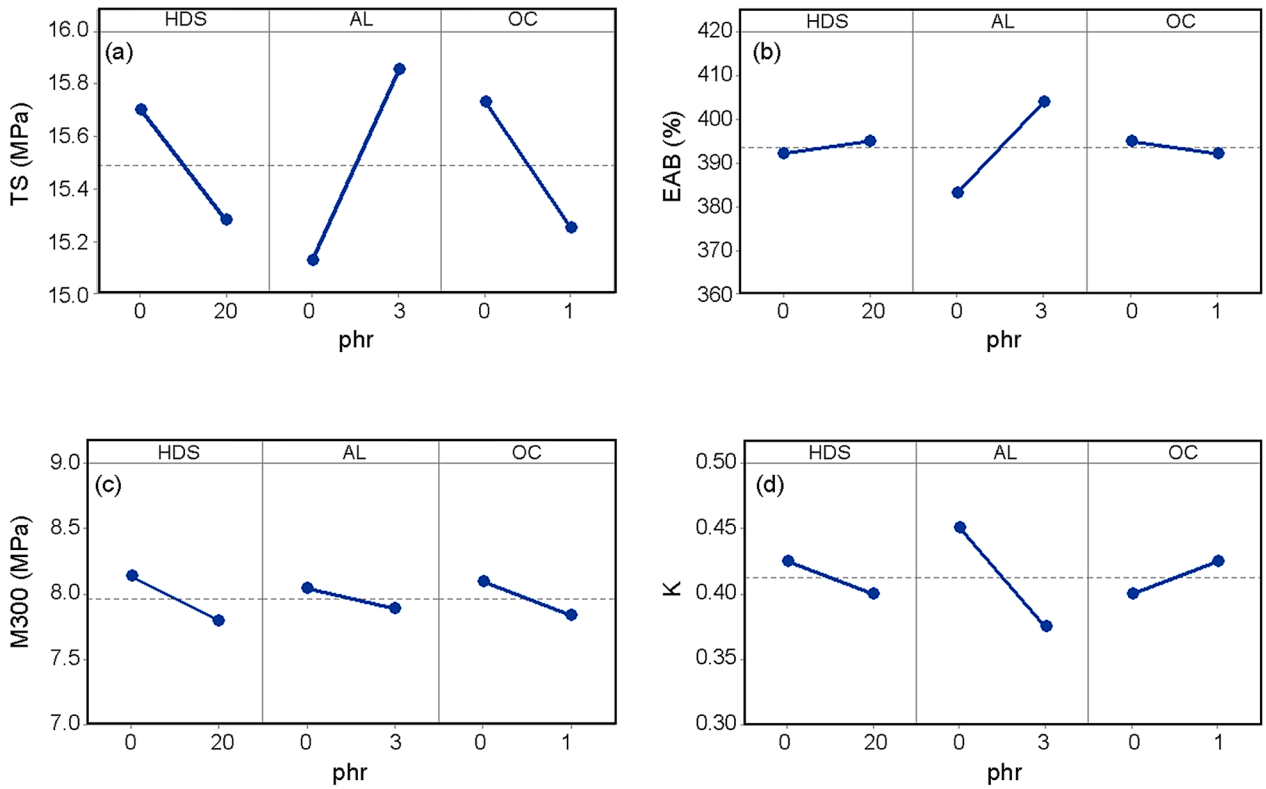


**Fig. 7** Main effects plots of filler concentration for (**a**) tensile strength force (TS), (**b**) elongation-at-break (EAB), (**c**) modulus 300% (M300) and (**d**) aging coefficient ($K$) of rubber composites

while AL and HDS show a decreasing effect on *K* by the decreases of curing rate.

## Failure properties and rubber composites hysteresis

Figure 8 shows the interaction effects plot for DeMatia crack growth of rubber composite. The developed model for this property is significant based on statistical analysis; the calculated *P* values of the model for DCG is 0.063 (Table 3). The coefficients of the regression model and the importance of each coefficient are also presented in Table 4.

It is evident from Fig. 8 that both silica and alumina show significant improving effects on the DeMatia crack growth. The DeMatia crack growth of elastomer composite depends on the modulus. Aure et al. showed that DeMatia crack growth resistance of carbon black-filled SBR composites decreases linearly with increase of modulus 300% [37]. So, part of this improvement behavior may be due to the reduced impact of these two mineral fillers on the rubber composite modulus. However, the changes in modulus are not significant compared to the significant improvement of DCG in the present study. The capacity to dissipate the stress concentration around the cracks is important for crack growth behavior of filled elastomers. Grosch et al. found that the hysteresis property is useful in estimating the relative strength of rubbers [38]. Dizon et al. showed that DeMatia crack growth of carbon black-filled SBR rubbers is very dependent on the carbon black structure and higher structure carbon blacks exhibited a significantly higher energy dissipative capacity and improved DeMatia crack growth behavior than their low structure counterparts [39]. Therefore, in the next step of the present study a dynamical mechanical analysis was conducted to better investigate the energy dissipative behavior of carbon black-filled composites in the

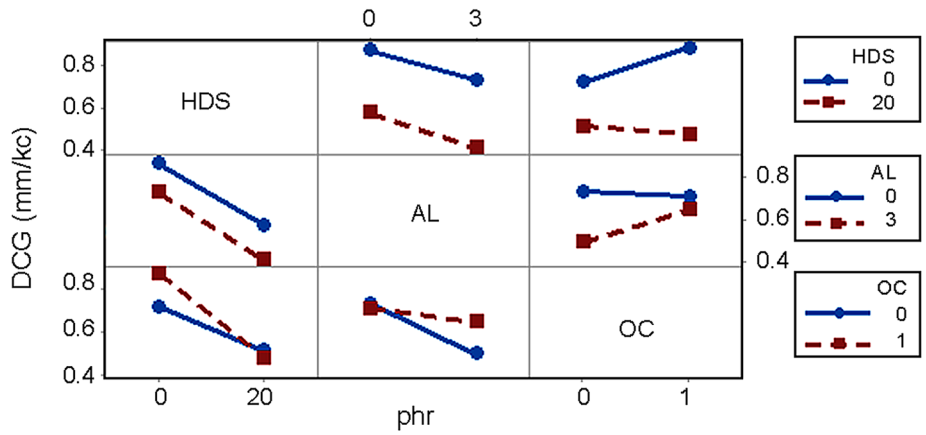


**Fig. 8** Interaction plots of filler concentration for DeMatia crack growth rate (DCG) of rubber composites

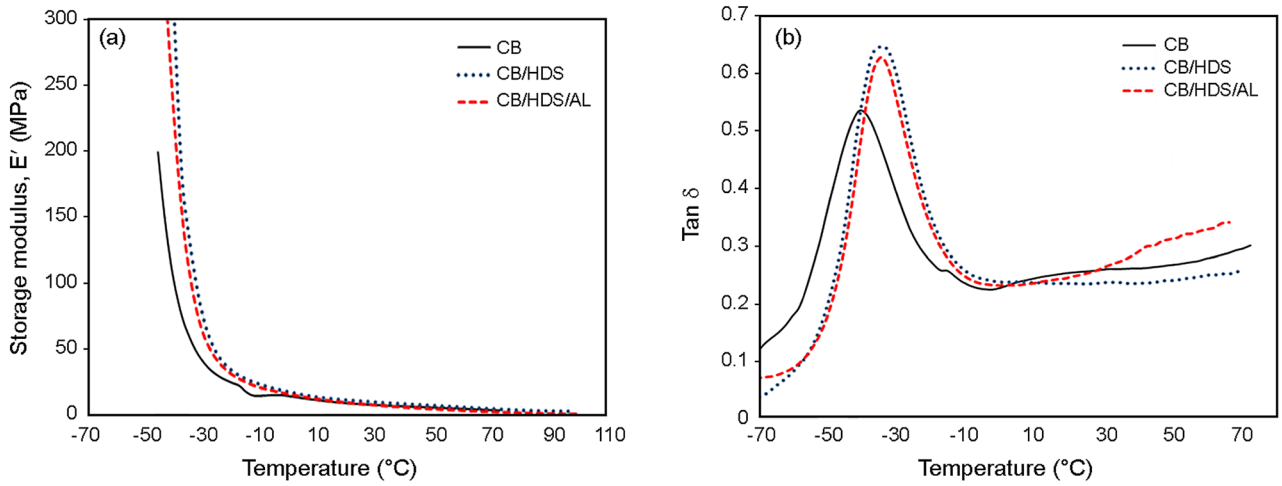


**Fig. 9** Temperature dependences of tan δ and storage modulus for carbon black-, carbon black/HDS- and carbon black/HDS/AL-filled tread composites

presence of mineral fillers. Figure 9 presents the temperature dependence of storage modulus and tan δ of composites filled with carbon black, carbon black/HDS and carbon black/HDS/AL. Tan δ is the ratio between loss modulus and elastic modulus. The loss modulus represents the viscous component of modulus and includes all the energy dissipation processes during dynamic strain. According to Fig. 9a, all composites show similar behavior in storage modulus at higher temperatures (rubbery state). The storage modulus of the vulcanizates in the rubbery state can be used to evaluate filler/filler interaction [6]. Figure 9a shows that compared to the carbon black-filled vulcanizate no severe agglomeration of filler nanoparticles or strong filler network structure may be formed in carbon black/HDS-filled and carbon black/HDS/AL-filled vulcanizates in the presence of silane coupling agent. Also, according to Fig. 9b, the tan δ peaks of the carbon black/HDS and carbon black/HDS/AL vulcanizates are higher than those of the carbon black vulcanizate, indicating that the filler network structure of carbon black/HDS and carbon black/HDS/AL vulcanizates are weaker than that of the carbon black vulcanizate. Because, it is well-known that in the glass transition zone, the main source of energy dissipation and hysteresis loss is from the polymer matrix and the filler network cannot be easily broken, so the weaker filler network structure leads to the higher tan δ peak [40]. In addition, according to Wang, at higher temperatures, where the polymer is in its rubbery state with very high entropic elasticity and low hysteresis, the cause of energy dissipation is related to the change of filler network structure during cyclic strain [8]. Therefore, at above 50 °C, where filler/filler interactions play dominant role in dissipative behavior of elastomer composites, carbon black/HDS/AL vulcanizates show again higher tan δ values, meaning that there are lower interparticle distances between fillers in this hybrid filler system compared to carbon black single filler system due to the presence of alumina particles along with high dispersible silica aggregates. So, better crack growth behavior of carbon black/HDS/AL ternary hybrid filler system may be attributed to its higher energy dissipative behavior compared to carbon black alone.

However, carbon black/HDS-filled composite (in the absence of alumina) exhibits less energy dissipative behavior, because lower values of loss factor at higher temperatures (above 50 °C, Fig. 9b) compared to carbon black-filled counterpart. Therefore, other mechanisms should be involved in improving crack growth behavior in the presence of silica, although, further study is needed to better understand the crack growth behavior of elastomer composites in the presence of mineral fillers: (1) by reducing curing rate due to loading silica and alumina, rubber fracture can be suppressed by a non-uniform stress distribution. It happens as a consequence of extended curing which results in a more homogeneous rubber composite as stated by Jeon et al. [35]; (2) crack growth resistance property of silica (and may be also alumina particles) as described by Bhattacharyya et al. which the silica particles due to their surface structure help to crack arresting [7] and (3) as stated in the previous sections, the improving effect of HDS and alumina on DCG may also be considered from the viewpoint of higher polysulfide crosslink density, which shows improving effects on crack growth behavior of the composites. The effect of crosslink density on fatigue crack growth behavior of rubber composites has been well described by Tse et al. [41]. The polysulfide crosslinks show better fatigue performance due to the breaking and reforming capability of cyclic deformations [41]. The statistical analysis of Table 4 for DCG shows that HDS × OC interaction term is statistically significant ($P$ value = 0.081). The interaction plots of Fig. 8 show that the crack growth of the composites is not influenced by OC in the presence of HDS, but it increases in the absence of HDS, although the modulus of the composite decreases by OC. This behavior may be also described through the effects of filler and silane coupling agent on the curing rate and type of sulfur crosslinks. The increasing effect of OC on DCG in the absence of HDS may be explained through the decreasing effect of OC on composite homogeneity and its increasing effect on the monosulfide crosslink density based on the increasing effect of OC on Pr. However, in the presence of silica/silane system with lower curing rates and higher content of polysulfide crosslinks and crack arresting capability of silica particles, the negative effect of OC on DCG is reduced.

The effect of the formula factors on the abrasion behavior of the rubber sample is shown in Fig. 10a and Table 4 (abrasion model). Interaction effects are statistically significant ($P$ values for $\beta_4$ and $\beta_6$ coefficients are 0.016 and 0.025, respectively, which are lower than 0.1, as in Table 4), and it complicates abrasion behavior. Abrasion resistance is a test of great importance as it can be related to the durability of tires. The effect of OC on abrasion behavior is not statistically significant ($P$ value of $\beta_3 = 0.126 > 0.1$, see Table 4). Mohanty et al. showed that partial replacement of carbon black with OC (3 and 5 phr) results in decreased resistance to abrasion of SBR composites [42]. Despite the use of a highly dispersible silica with high surface area and the presence of silane coupling agent as an efficient surface modifier, a relatively slight increase (but statistically significant) in DIN abrasion by silica may be confirmed by the regression model for abrasion ($P$ value of $\beta_1 = 0.03 < 0.1$, Table 4) and interaction plots of Fig. 10a.

The observed decrease in abrasion resistance is in agreement with the change in glass transition temperature ($T_g$) of carbon black-filled SBR composite in presence of mineral fillers as shown in Fig. 9b. The $T_g$ of carbon black/HDS and carbon black/HDS/AL filler systems has increased compared to the $T_g$ of carbon black counterpart. Keinel and

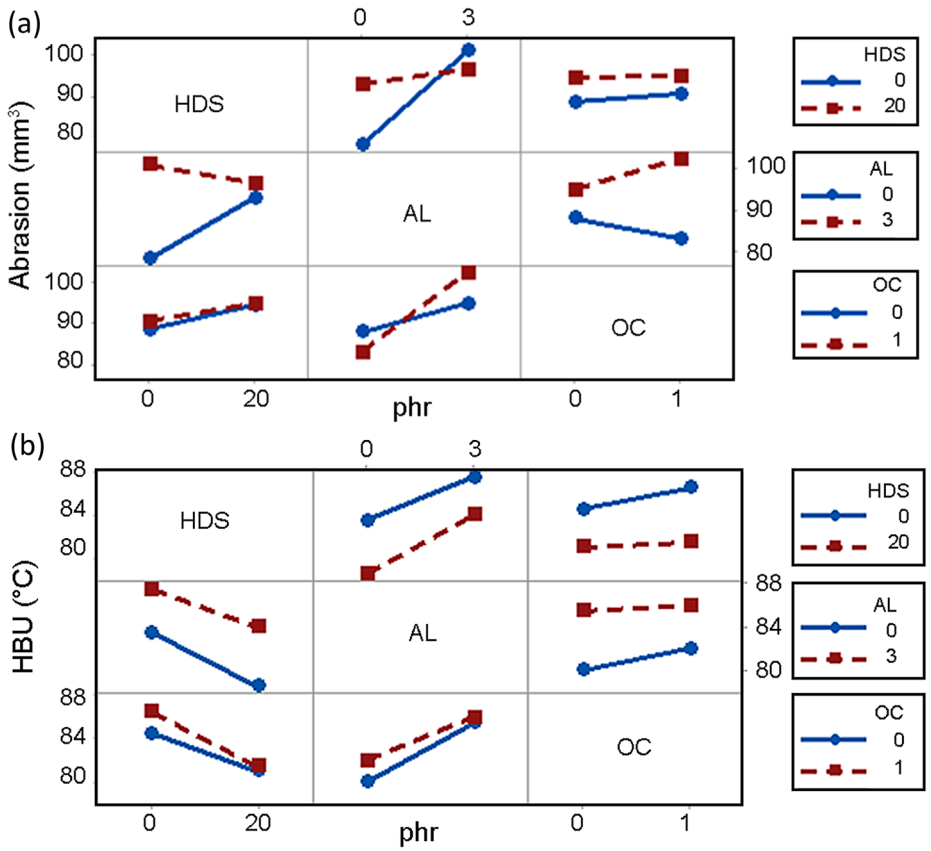


**Fig. 10** Interaction plots of filler concentration for (**a**) abrasion and (**b**) heat buildup of rubber composites

Dizon showed that the polymers with higher $T_g$ give greater abrasion loss or poorer abrasion resistance [43].

A good comparison between high dispersible silica (Z1165 MP) and carbon black performance on the abrasion behavior of SBR and SBR/BR tread tire composites presented by Wu showed that carbon black-filled rubber was more susceptible to smearing wear than the silica-filled rubber, and during mechano-chemical degradation a sticky layer was generated on the rubber surface [44]. This behavior is called "smearing wear" with an improving effect on abrasion behavior [44].

Alumina shows an increasing effect on abrasion (Fig. 10a). This effect may be due to some large agglomerates that are formed along with very fine nanoparticles as depicted in Fig. 2c. Figure 10a also shows that the negative effect of alumina on the abrasion decreases in the presence of silica. The abrasion behavior of the rubber is significantly dependent on the dispersion degree of the filler and rubber composite modulus [45, 46]. Because minor amounts of silane have been used in silica formulas, it is likely that the silane coupling agent would improve the alumina surface and its dispersion [17]. These interaction effects were more reflective in the abrasion properties. Wang et al. proposed a modification plan of the alumina surface during mixing with the silane coupling agent [17]. Under the shear stress and high temperature of mixing process, the silane coupling agent TESPT will be firstly grafted on the surface of alumina particles through the condensation reaction between the hydroxyl group on the alumina surface and ethoxy group of silane. In the next step, the reaction between surface-modified alumina and rubber chains occurs through the sulfur coupling during the curing process. So, possibly better dispersion and strong chemical coupling between alumina and rubber can have a beneficial effect on abrasion behavior [47].

The Goodrich heat buildup of composites is presented in Fig. 10b. The regression model based on factor variables and their significance is presented in Table 4. Alumina incremental behavior and silica reduction behavior on HBU are both statistically significant according to the coefficients of $\beta_1$ and $\beta_2$ for HBU (Eq. 5) which are −2.125 and 2.375 with corresponding $P$ values of 0.037 and $0.033 < 0.1$, respectively. However, the coefficient of $\beta_3$ for HBU model (Eq. 5) is 0.625 with corresponding $P$ value of $0.126 > 0$, indicating the increasing effect of OC which is not significantly important.

Silica reduces the rubber composite heat buildup. This is the expected behavior of silica in the replacement of carbon black, which has been addressed at several references [10, 48]. The heat buildup result of silica is in agreement with the loss factor (Tan δ) result at temperatures above

50 °C (Fig. 9b). Both behaviors may be due to lower filler/filler interactions as discussed previously according to the Wang statements [8]. In addition, it is important to note that improvement of the rubber heat build-up by partial substitution of carbon black with highly dispersible silica in the presence of silane coupling agent is better to be explained by the reduction of filler/rubber interactions rather than filler/filler interactions, as discussed by Byers [10]. He stated that the primary contributor to make differences in Payne effect in filled rubber systems is the adsorption/desorption of polymeric chains at the interface (filler/polymer interaction) rather than a filler network effect.

In agreement with Tan δ results at temperatures above 50 °C (Fig. 9b), alumina shows an incremental effect on the heat build-up behavior, that confirms again the increase of energy dissipative behavior of the composites in presence of alumina particles. The OC shows a slight incremental behavior on rubber heat build-up. Statistical analysis of Table 4 does not consider this behavior to be statistically significant. The increase of HBU in SBR tire tread formulation as the carbon black is increasingly replaced by OC is also reported by Mohanty et al. [42], because the possibility of fillers-OC interface formation should be increased, leading to increase in inter-filler friction which ultimately results in loss of energy in the form of heat as stated by Mohanty et al. [42]. The increasing effect of OC on hysteresis of SBR and BR rubber composites has been also reported by Ganter et al. [31].

## Thermal conductivity behavior

Figure 11 shows the dependence of thermal diffusion coefficient (Alpha) on three variables, OC, silica and alumina contents by which all three factors have incremental effects on this coefficient. Statistical analysis of Table 4 shows that the effect of all three variables is statistically significant ($\beta_1 = 0.1875$ with $P$ value $= 0.042 < 0.1$, $\beta_2 = 0.1625$ with $P$ value $= 0.049 < 0.1$ and $\beta_3 = 0.1125$ with $P$ value $= 0.07 < 0.1$ for Alpha regression model). Also, the interaction effects of silica-organoclay and silica-alumina are significant ($\beta_4 = 0.0875$ with $P$ value $= 0.09 < 0.1$ and $\beta_5 = -0.2125$ with $P$ value $= 0.037 < 0.1$).

The size and shape of the filler, the thermal conductivity of the filler, the filler/polymer interaction, the filler agglomeration and free volume influence the thermal conductivity behavior of the polymer nanocomposites as stated by Tsekmes et al. [3]. Therefore, in the present study, the improving effect of mineral fillers on heat conductivity may be described according to the following interconnected important phenomena: (1) the distance between filler particles that depends on filler content and filler dispersion and agglomeration state in rubber matrix and (2) phonon scattering phenomena that it is very dependent on filler/rubber interactions. As it is clearly presented in Fig. 3, comparing with carbon black-filled composites (Fig. 3f), the distance between fillers has been decreased in a mixture of carbon black and mineral fillers (Fig. 3e). Gua et al. in their review article stated that the use of a hybrid filler (two or more fillers alongside each other) has a significant synergistic effect in increasing the thermal conductivity of the polymer [1], and the presence of alumina particles along with coarse fillers has led to a significant increase in composite thermal conductivity. The finer particles can be located between the coarse particles and cause uniformity in the direction of heat conduction [1, 4]. Increasing the rubber thermal conductivity with the presence of alumina particles can be attributed to the high thermal conductivity of these particles and their appropriate morphology in the rubber matrix (Fig. 2b). The improvement of rubber thermal conductivity in the presence of alumina has been reported by some researchers [16, 17]. Li et al. have shown that the heat conductivity of gum ESBR can be increased by 60% by adding 100 phr of micro

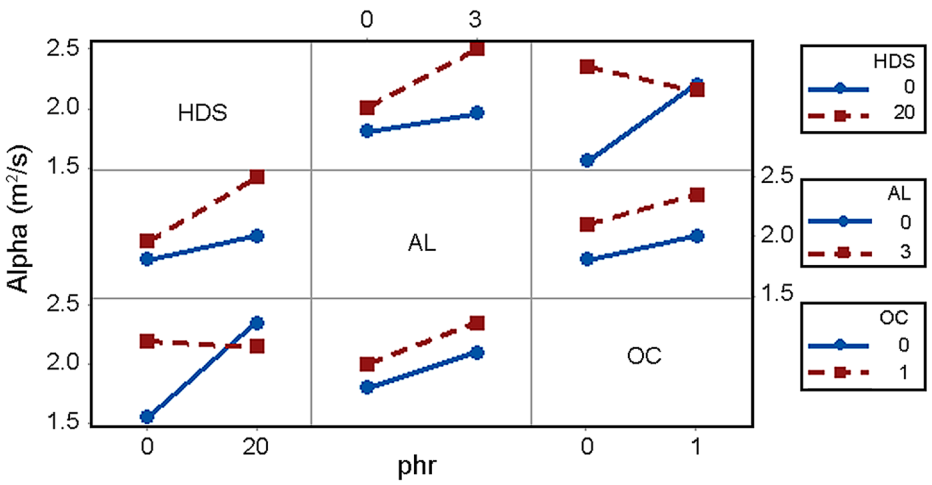


**Fig. 11** Interaction plots of filler concentration for thermal diffusivity coefficient of rubber composites

size alumina particles [16]. Compared to 20% by volume of carbon black- and silica-filled EPDM composites, a 50% increase in thermal conductivity of EPDM rubber has been reported in the presence of 20% by volume of alumina nanoparticles [17]. Han et al. also reported a 20% of increase in the thermal conductivity of the epoxy composite in the presence of alumina filler agglomerates [49]. The relatively similar improvements of heat conductivity behavior (about 50% increase of Alpha) are evidenced in the present study with quaternary hybrid filler system of alumina besides carbon black, HDS and OC. It has been reported that the agglomeration of the filler particles increases the composite thermal conductivity [3]. Evans et al. modeled the role of agglomerates in thermal conductivity behavior [50]. So, increasing the rubber thermal conductivity by replacing part of the carbon black with silica can be attributed to the creation of more agglomerates or a filler network with closer particles by this filler (Figs. 2, 3d, e), which increases the conduction paths of heat. According to DMA and microscopic results of the present study, there is no severe agglomeration in carbon black/HDS/Al hybrid filler system, but the fillers are closer to each other compared to carbon black filler system.

Ghoreyshy and Abbassi-Sourki have shown the important contribution of silica dispersion to rubber thermal diffusion coefficient [22]. The use of solution SBR instead of emulsion SBR results in better silica dispersion and reduces rubber thermal conductivity, probably due to the decrease of heat conductive paths. It is worth mentioning that in the above article [22], the Alpha of carbon black-filled emulsion SBR composite (measured at 130 °C) has been improved by about 25% using HDS/carbon black binary filler system. However, an improvement of more than 50% in heat diffusivity coefficient of carbon black-filled emulsion SBR composite is observed in the presence of quaternary hybrid filled system of the present study.

Regarding the improving effect of OC on the rubber thermal diffusion coefficient as presented in Fig. 11, it can also be noted that, according to the references [50, 51], the high-aspect ratio plate fillers show a positive effect on the thermal conductivity behavior of the polymer. Because the high aspect ratio can favor the formation of heat conduction networks by reducing the percolation threshold and the interfacial thermal resistance [50, 51]. The impact of the clay filler on the free volume of rubber or in other words the thermal conductivity coefficient has also been reported. Roy et al. studied three different modes of polymer–clay nanocomposite, in which the free volume was reduced [52]. It is believed that the filler/rubber interactions affect the thermal conductivity [1, 3]. Better adhesion and bonding between the filler and the polymer can reduce the phonon scattering and improve thermal conductivity [1, 4]. The effect of using coupling agents to improve the thermal conductivity of filled composites is well reviewed [1, 3]. The interaction effects curve presented in this article suggests that in the presence of a silane coupling agent, alumina is more effective on thermal conductivity. Basically, according to existing references [10, 17], the modification of the silica and alumina with the silane coupling agent causes a better filler/rubber interaction, which has a positive effect on the thermal conductivity behavior by reducing the phonon scattering [1, 4]. Sarkawi et al. portrayed voids in the silica-rubber interfaces during the study of silica dispersion in the NR matrix without a coupling agent that was carried out by TEM [53]. These voids are the result of a weak interaction of silica/rubber, which can have a negative effect on rubber thermal conductivity. Therefore, the role of the silane coupling agent factor and the modification of silica or alumina surface, which increases the interaction of filler/rubber and the reduction of cavities, is very important [53]. Also, the correction of the nanoparticle surface provides the potential for reducing the free volume of the composite, since the formation of chemical bonds at the surface of the filler/rubber contact reduces the interfacial density and minimizes imperfections such as microcavities [53].

## Optimal formula development

The results from Table 2 show that Mix 6 composite including ternary filler system (carbon black = 33, HDS = 20, AL = 3 and OC = 0 phr) and Mix 7 composite including quaternary filler system (carbon black = 33, HDS = 20, AL = 3 and OC = 1 phr) have the highest heat diffusivity coefficients and the best crack growth behavior, keeping the same values of modulus, hardness, HBU and resilience. However, T90 for Mix 6 composite is higher than the reference carbon black-filled composite (Mix 5) with a slight increase in DIN abrasion. T90 for Mix 7 composite is decreased due to the presence of OC, whereas its DIN abrasion is high. Hereafter, a multi-objective optimization on the basis of desirability function approach has been conducted with the aid of factorial response optimizer tools of MINITAB software to achieve the best conditions of HDS, AL and OC according to regression models for key composite properties. The use of optimization algorithms in DOE studies on the basis of regression polynomial models has been well addressed [27, 54]. The approach of desirability function is widely used in industry for the optimization of multiple response processes [54].

The optimal formulation has been presented in Table 5 that proposes the replacement of 20 phr of carbon black by 20 phr of silica, besides adding 0.5 phr of modified layered silicate and 1.2 phr alumina filler. Five key properties with statistically significant regression model were considered to develop an optimal formulation. The expected properties as well as the experiment results for the proposed optimal formula are presented in Table 5. In the last column of the

**Table 5** Formula optimization

| | Optimum formula[a] | Reference |
|---|---|---|
| HDS (phr) | 20 | 0 |
| AL (phr) | 1.2 | 0 |
| OC (phr) | 0.5 | 0 |
| Abrasion ($mm^3$) | 93 (94.374 ± 0.2299) | 80 |
| DCG (mm/kc) | 0.50 (0.51071 ± 0.11493) | 0.84 |
| HBU (°C) | 81 (80.649 ± 0.2299) | 82 |
| Alpha ($m^2/s$) | 2 (2.1967 ± 0.2299) | 1.5 |
| T90 (min) | 24.7 (24.996 ± 0.1655) | 26.45 |

[a]The values in parentheses are data predicted from regression models

table, the properties of the reference composite are given for comparison (Mix 5). The results of Table 5 (experiments and predicted values) show that the optimal formula has much better DeMatia crack growth than carbon black reference formula, and only a slight decrease is observed in the abrasion behavior. The thermal diffusion coefficient of the composite is higher than that of the reference sample and the optimal curing time of the composite is lower than that of the carbon black reference. Kim et al. stated that composites manufactured by ternary filler system using carbon black, silica (HDS) and OC based on 100 phr SBR have a potential for tire tread applications [13]. The present study also reveals the potential to develop a heat conductive tire tread composite using the above ternary filler system along with heat conductive reinforcing filler such as nanoalumina.

## Conclusion

The effects of quaternary filler composite including carbon black, high dispersible silica, modified layered silicate and alumina alongside the silane coupling agent in SBR/BR blend used in a tread tire were studied. An optimum formulation was developed with better crack growth properties, higher thermal conductivity and lower sulfur curing time compared to carbon black tire tread composite.

From the viewpoint of transport phenomena, the SBR/BR composite thermal conductivity coefficient was improved significantly by applying this new filler system. Therefore, it is expected that the temperature of the thick parts, such as tread, will increase faster during the sulfur curing process, which will decrease the time required to cure the piece and also will result in the more uniform distribution of the properties in different points of the rubber parts.

From the sulfur curing kinetics point of view, the faster sulfur curing of this composite is the other advantage of the use of quaternary filler blend, which is again in line with the goals of reducing the rubber curing time, reducing production costs along with maintaining product quality. It is also important to reduce the rubber curing time from the environmental point of view, as well as to reduce the carbon black contribution in the filler system and replacing it with white ecofriendly fillers which is the other positive environmental aspect of this composite.

Finally, from a performance viewpoint, a composite with improved crack growth and a rather weaker abrasion behavior has been developed that it is meant to further study and predict its performance on road.

**Acknowledgements** The authors of this article are grateful for financial support and services from Kavir Tire Company.

## References

1. Guo B, Tang Z, Zhang L (2016) Transport performance in novel elastomer nanocomposites: mechanism, design and control. Prog Polym Sci 61:29–66
2. Li A, Zhang C, Zhang YF (2017) Thermal conductivity of graphene-polymer composites: mechanisms, properties, and applications. Polymers 9:437–454
3. Tsekmes I, Kochetov R, Morshuis P, Smit J (2013) Thermal conductivity of polymeric composites: a review. In: IEEE International Conference on Solid Dielectrics (ICSD). Paper presented at 2013
4. Guo Y, Ruan K, Shi X, Yang X, Gu J (2020) Factors affecting thermal conductivities of the polymers and polymer composites: a review. Compos Sci Technol 193:108–134
5. Wypych G (2000) Handbook of fillers, 2nd edn. ChemTec Publishing, Toronto
6. Li Y, Han B, Liu L, Zhang F, Zhang L, Wen S, Shen J (2013) Surface modification of silica by two-step method and properties of solution styrene butadiene rubber (SSBR) nanocomposites filled with modified silica. Compos Sci Technol 88:69–75
7. Bhattacharyya S, Dasgupta S, Londa V, Mukhopadhyay R (2019) Influence of highly dispersible silica filler on the physical properties, tearing energy and abrasion of tire tread compound. J Appl Polym Sci 136:47560–47572
8. Wang MJ (1998) Effect of polymer-filler and filler-filler interactions on dynamic properties of filled vulcanizates. Rubber Chem Technol 71:520–589
9. Wagner MP (1976) Reinforcing silicas and silicates. Rubber Chem Technol 49:703–774
10. Byers JT (2002) Fillers for balancing passenger tire tread properties. Rubber Chem Technol 75:527–548
11. Galimberti M, Agnelli S, Cipolletti V (2017) In: Thomas S, Maria HJ (eds) Progress in rubber nanocomposites, Woodhead Publishing, UK
12. Rooj S, Das A, Morozov IA, Stöckelhuber KW, Stocek R, Heinrich G (2013) Influence of expanded clay on the microstructure and fatigue crack growth behavior of carbon black filled NR composites. Compos Sci Technol 76:61–68
13. Kim WS, Lee DH, Kim IJ, Son MJ, Kim W (2009) SBR/organoclay nanocomposites for the application on tire tread compounds. Macromol Res 17:776–784
14. Arroyo M, López-Manchado M, Herrero B (2003) Organo-montmorillonite as substitute of carbon black in natural rubber compounds. Polymer 44:2447–2453
15. Mohan TP, Kuriakose J, Kanny K (2011) Effect of nanoclay reinforcement on structure, thermal and mechanical properties

of natural rubber–styrene butadine rubber (NR–SBR). J Ind Eng Chem 17:264–270
16. Li Z, Chen H, Zhu Z, Zhang Y (2011) Study on thermally conductive ESBR vulcanizates. Polym Bull 67:1091–1104
17. Wang ZH, Lu YL, Liu J, Dang ZM, Zhang LQ, Wang W (2011) Preparation of nanoalumina/EPDM composites with good performance in thermal conductivity and mechanical properties. Polym Adv Technol 22:2302–2310
18. Roy K, Jatejarungwong C, Potiyaraj P (2018) Development of highly reinforced maleated natural rubber nanocomposites based on sol-gel-derived nano alumina. J Appl Polym Sci 135:46248–46257
19. Teena T, Ayswarya EP, Eby TT (2013) Nano alumina as reinforcement in natural rubber composites. Int J Innov Res Sci Eng Technol 2:2365–2370
20. Ten Brinke J, Debnath S, Reuvekamp LA, Noordermeer JW (2003) Mechanistic aspects of the role of coupling agents in silica–rubber composites. Compos Sci Technol 63:1165–1174
21. Gabriel CFS, Gabino AAP, de Sousa AMF, Furtado CRG, Nunes RCR (2019) Tire tread rubber compounds with ternary system filler based on carbon black, silica, and metakaolin: contribution of silica/metakaolin content on the final properties. J Elast Plas 51:712–726
22. Ghoreishy MHR, Abbassi-Sourki F (2017) The molecular structure of SBR and filler type effects on thermal diffusivity of SBR/BR compounds used in tire tread. (in persian) Iran. J Polym Sci Technol 30:139–149
23. Pan Q, Wang B, Chen Z, Zhao J (2013) Reinforcement and antioxidation effects of antioxidant functionalized silica in styrene–butadiene rubber. Mater Des 50:558–565
24. Limrungruengrat S, Chaikittiratana A, Pornpeerakeat S, Chantrasmi T (2018) Finite element analysis for evaluation of cure level in a large rubber part. Mater Today Proc 5:9336–9343
25. Hands D (1977) The thermal transport properties of polymers. Rubber Chem Technol 50:480–522
26. Proust M (2005) Design of experiments. SAS Institute Inc, Cary
27. Derringer GC (1988) Statistical methods in rubber research and development. Rubber Chem Technol 61:377–421
28. Ghasemi I, Karrabi M, Mohammadi M, Azizi H (2010) Evaluating the effect of processing conditions and organoclay content on the properties of styrene-butadiene rubber/organoclay nanocomposites by response surface methodology. Exp Polym Lett 4:62–70
29. Balachandran M, Bhagwan SS, Muraleekrishnan R (2011) Modeling and optimizing properties of nanoclay–nitrile rubber composites using Box-Behnken Design. Rubber Chem Technol 84:455–473
30. Choi SS, Choi SJ (2006) Influence of silane coupling agent content on crosslink type and density of silica-filled natural rubber vulcanizates. Bull Korean Soc 27:1473–1476
31. Ganter M, Gronski W, Reichert P, Mülhaupt R (2001) Rubber nanocomposites: morphology and mechanical properties of BR and SBR vulcanizates reinforced by organophilic layered silicate. Rubber Chem Technol 74:221–235
32. Bhattacharya M, Maiti M, Bhowmick AK (2008) Influence of different nanofillers and their methods on the properties of natural rubber nanocomposites. Rubber Chem Technol 81:782–808
33. Custodero E, Tardivat JC (1999) Diene rubber composition based on alumina as reinforcing filler and it's use for the manufacture of a tire. Patent US005900449A
34. Gherib S, Chazeau L, Pelletier JM, Satha H (2010) Influence of the filler type on the rupture behavior of filled elastomers. J Appl Polym Sci 118:435–445
35. Jeon GS, Han MH, Seo G (1999) Enhancing adhesion properties between rubber compound and brass-plated steel cord by incorporating silica into rubber. J Adhesion Sci Technol 13:153–168
36. Datta RN (2003) Review on heat and reversion resistance compounding. Prog Rubber Plast Re 19:143–170
37. Auer EE, Doak KW, Schaffner IJ (1958) Factors affecting laboratory cut-growth resistance of cold SBR tread stocks. Rubber Chem Technol 31:185–201
38. Grosch K, Harwood JAC, Payne AR (1966) Breaking energy of rubbers. Nature 212:497
39. Dizon ES, Hicks AE, Chirico VE (1973) The effect of carbon black parameters on the fatigue life of filled rubber compounds. Rubber Chem Technol 47:231–249
40. Robertson CG, Lin CJ, Rackaitis M, Roland CM (2008) Influence of particle size and polymer–filler coupling on viscoelastic glass transition of particle-reinforced polymers. Macromolecules 41:2727–2731
41. Tse MF, Mcelrath KO, Wang HC (2002) Relating De Mattia cut growth to network structure of crosslinked elastomers. Polym Eng Sci 42:1210–1219
42. Mohanty TR, Bhandari V, Chandra AK, Chattopadhyay PK, Chattopadhyay S (2013) Role of calcium stearate as a dispersion promoter for new generation carbon black-organoclay based rubber nanocomposites for tyre application. Polym Compos 34:214–224
43. Kienle RN, Dizon ES (1971) Tread wear and wet skid resistance of butadiene-styrene elastomers. Rubber Chem Technol 44:996–1014
44. Wu G (2016) The mechanisms of rubber abrasion. Phd thesis, Queen Mary University of London
45. Rattanasom N, Saowapark T, Deeprasertkul C (2007) Reinforcement of natural rubber with silica/carbon black hybrid filler. Polym Test 26:369–377
46. Fukahori Y, Yamazaki H (1995) Mechanism of rubber abrasion part 3: how is friction linked to fracture in rubber abrasion? Wear 188:19–26
47. Shiva M, Hadadi AH, Nakhaei A, Varasteh H (2015) Study of abrasion of rubber materials by experimental design, response surface and artificial neural network nodeling (in persian) lran. J Polym Sci Technol 28:197–209
48. Ma JH, Zhao SH, Zhang LQ, Wu YP (2013) Comparison of structure and properties of two styrene–butadiene rubbers filled with carbon black, carbon-silica dual phase filler, and silica. Rubber Chem Technol 86:664–678
49. Han Z, Wood JW, Herman H, Zhang C, Stevens GC (2008) Thermal properties of composites filled with different fillers. In: Conference Record of the 2008 IEEE International Symposium on Electrical Insulation, IEEE, pp. 497–501
50. Evans W, Prasher R, Fish J, Meakin P, Phelan P, Keblinski P (2008) Effect of aggregation and interfacial thermal resistance on thermal conductivity of nanocomposites and colloidal nanofluids. Int J Heat Mass Transf 51:1431–1438
51. Kochetov R, Korobko AV, Andritsch T, Morshuis PHF, Picken SJ, Smit JJ (2011) Modelling of the thermal conductivity in polymer nanocomposites and the impact of the interface between filler and matrix. J Phys D Appl Phys 44:395–401
52. Roy M, Nelson JK, MacCrone RK, Schadler LS, Reed CW, Keefe R, Zenger W (2005) Polymer nanocomposite dielectrics-the role of the interface. IEEE T Dielect El In 12:629–643
53. Sarkawi SS, Dierkes WK, Noordermeer JWM (2014) Elucidation of filler-to-filler and filler-to-rubber interactions in silica-reinforced natural rubber by TEM network visualization. Eur Polym J 54:118–127
54. Krajnik P, Kopac J, Sluga A (2005) Design of grinding factors based on response surface methodology. J Mater Proc Technol 162–163:629–636